North Atlantic summers have warmed more than winters since 1353, and the response of marine zooplankton

Nicholas A. Kamenos[1]

School of Geographical and Earth Sciences, University of Glasgow, Glasgow G12 8QQ, Scotland

Edited by Edward A. Boyle, Massachusetts Institute of Technology, Cambridge, MA, and approved November 2, 2010 (received for review May 3, 2010)

Modeling and measurements show that Atlantic marine temperatures are rising; however, the low temporal resolution of models and restricted spatial resolution of measurements (*i*) mask regional details critical for determining the rate and extent of climate variability, and (*ii*) prevent robust determination of climatic impacts on marine ecosystems. To address both issues for the North East Atlantic, a fortnightly resolution marine climate record from 1353–2006 was constructed for shallow inshore waters and compared to changes in marine zooplankton abundance. For the first time summer marine temperatures are shown to have increased nearly twice as much as winter temperatures since 1353. Additional climatic instability began in 1700 characterized by ∼5–65 year climate oscillations that appear to be a recent phenomenon. Enhanced summer-specific warming reduced the abundance of the copepod *Calanus finmarchicus*, a key food item of cod, and led to significantly lower projected abundances by 2040 than at present. The faster increase of summer marine temperatures has implications for climate projections and affects abundance, and thus biomass, near the base of the marine food web with potentially significant feedback effects for marine food security.

coralline algae | rhodolith | maerl | seasonal

Prior to instrumentally derived temperature records that began in the 1850s, knowledge of seasonal and regional-scale marine temperature changes at high latitudes is limited. Thus at present, hemispheric Atlantic climatic patterns are deduced from multiproxy and instrumental networks using statistical (1, 2) and modeling (3) approaches. Whereas such approaches show that the Atlantic Multidecadal Oscillation (AMO), the North Atlantic Oscillation (NAO), and Atlantic Meridional Overturning Circulation (AMOC) have a substantial influence on Atlantic climate (e.g., ref. 4) they are still unable to capture details that are critical for determining the spatiotemporal distribution of climate oscillations (5, 6) and their associated impacts (7). For example, whereas the AMO, which models suggest reflects multidecadal variation in the AMOC (8), is the dominant influence on summer climate in the United Kingdom (9), at higher European latitudes, seasonal terrestrial tree-ring climate records (6, 10) are not representative of high-latitude sea surface temperatures (11). Limited spatiotemporal resolution, absent proxy validation and organism effects have restricted the distribution of current inshore proxy-derived sea surface temperature (SST) records (12–16). Therefore to date, we have a poor understanding of season specific temperature variability. Similarly, SST, AMO, and AMOC variations are not well represented at high spatiotemporal resolution beyond the instrumental record in North East Atlantic shallow inshore waters (for example 55°50'N 05°50'W). This information is needed to better understand rates of regional climate variability (5).

Marine responses to such climate fluctuations are reflected in the productivity of marine ecosystems from phytoplankton to fish population dynamics (17). Therefore a key requirement for preserving biodiversity and supporting sustainable fishing is to understand the climatic effects in the lower levels of food webs (18). At present, general circulation models treat the marine environment in a simplified way, lacking the detail required for investigating the impacts of climate on marine ecosystems (7) beyond phytoplanktonic trophic levels. Thus the utility of high resolution marine temperature histories coupled with seasonal records of productivity provide a unique tool for probing climate-marine ecosystem relationships more accurately. With models suggesting that Atlantic SST will continue to rise (19) we need to understand how such changes are likely to affect food security.

The first biweekly resolution record of high-latitude, North East Atlantic, inshore, shallow-water temperature from 1353–2006 is presented and related to seasonal resolution inshore zooplankton changes. Mg/Ca ratios obtained from red coralline algae (*Lithothamnion glaciale*) were converted to in situ marine temperatures using Mg-temperature calibrations performed here and in ref. 20. Red coralline algae are validated (14) archives of palaeoclimate information at subannual time scales (20, 21), which band annually (20, 22) and have a worldwide shallow-water distribution (23). As zooplankton amplify hydroclimatological forcing (24) this investigation targeted historic relationships between North East Atlantic algae-derived in situ temperatures and abundances of the copepod *Calanus finmarchicus*, the most abundant copepod species higher than 50° N (25) and an important food source for cod (26). East Atlantic *C. finmarchicus* abundance was related to algae-derived in situ temperature and that relationship along with model-derived temperature projections (19) were used to project *C. finmarchicus* abundance to 2040.

Results and Discussion

Since the Little Ice Age (LIA) summer marine temperatures in North East Atlantic inshore shallow waters have increased nearly twice as much as those in winter. From the LIA [1400–1700 (27)] to the 1900–2006 mean, summer temperatures rose by 2.7± 0.5 °C while winter temperatures rose by 1.4 ± 0.5 °C (Fig. 1). This seasonal difference in change may be attributed either to (*i*) more suppressed summer than winter temperatures during the LIA or (*ii*) that since the LIA summers have warmed more than winters. In both cases, summers have warmed more than winters during the last 6 centuries.

Temperature peaks near ∼1350, 1700, 1870, 1920, and since the 1970s are similar to present day SSTs. Distinct temperature troughs occurred near ∼1540, 1840, 1880, and 1960. In fact, since 1930 the mean temperatures have been significantly higher than the 1353–1929 summer ($F_1 = 50.62$, $p < 0.001$) and winter ($F_1 = 78.39$, $p < 0.001$) temperatures respectively.

Author contributions: N.A.K. designed research, performed research, analyzed data, and wrote the paper.

The author declares no conflict of interest.

This article is a PNAS Direct Submission.

[1]E-mail: nick.kamenos@glasgow.ac.uk.

This article contains supporting information online at www.pnas.org/lookup/suppl/doi:10.1073/pnas.1006141107/-/DCSupplemental.

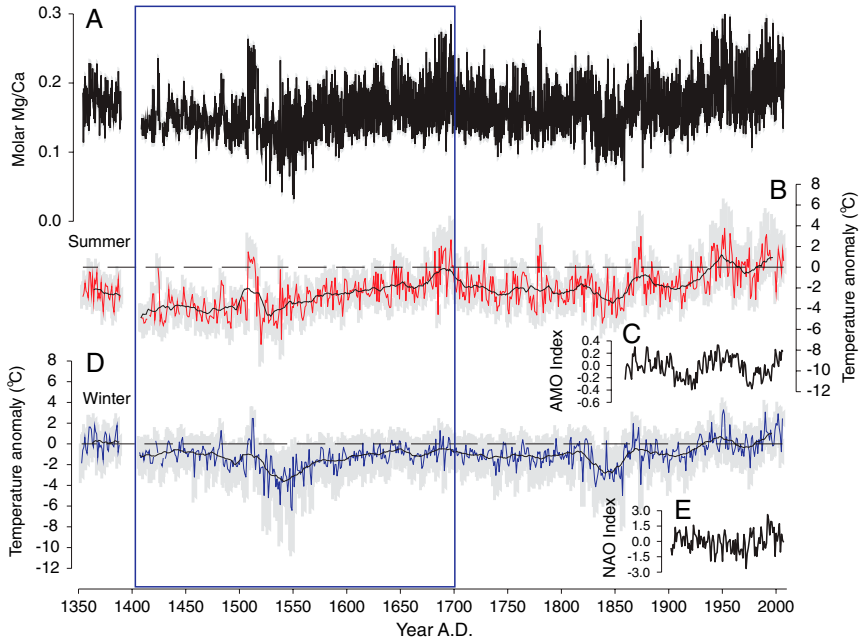

Fig. 1. North East Atlantic summer and winter algae-derived in situ temperature anomaly. Molar Mg/Ca (black line) extracted from *L. glaciale* coralline algae on the west coast of Scotland (graph *A*), peaks represent maximum summer temperature and troughs minimum winter temperature. Gray shading indicates Mg/Ca SD of replicate measurements. Summer (graph *B*—red line) and winter (graph *D*—blue line) extreme algae-derived temperature anomalies were extracted from the fortnightly resolution subannual time series. Gray shading indicates standard error (measurement and regression) and black line indicates 21 year moving average. Blue box indicates temporal extent of the LIA as defined by (27). The winter Atlantic Multidecadal Oscillation (AMO) index (Raw data from ref. 38) (graph *C*) and winter (December-March) North Atlantic Oscillation (NAO) index (principal component from ref. 45) (graph *E*) are indicated.

Maximum offsets since 1353 with respect to the 1961–1990 mean algae-derived in situ temperature (11.5 ± 0.5 °C) were greater in winter (-8.9 ± 0.5 °C) than summer ($+6.3 \pm 0.5$ °C). Whereas this does not indicate consistently larger changes in winter temperature, it does indicate that even though summer marine temperatures have on average increased more, winter marine temperatures have been characterized by more extreme temperatures as also observed in terrestrial alpine temperature reconstructions (1, 6).

The distinct period of cooler temperatures between ~1418 and the late 1600s coincides with the LIA that reached spatially distinct minima in the Northern hemisphere between 1400–1700 (27). The LIA was characterized by both warm and cold anomalies (28) such as the distinct positive temperature deviation that occurs between ~1506–1516 and is present in both summer and winter. As these cooling and warming periods correspond to similar periods observed in marine and terrestrial multi- and single-proxy reconstructions (e.g., refs. 1 and 27–29), as well as climate indices (30, 31), it appears that shallow inshore waters are experiencing environmental conditions characteristic of both deeper offshore waters as well as the atmosphere. Therefore, these data suggest that the shallow inshore waters in Loch Sween are representative of larger-scale climatic variability. The presence of live coralline algae indicates that, at least in the Loch Sween system, during the LIA these sea lochs were not frozen, although there may have been surface ice present during winter. Such surface ice would not have led to algal growth cessation as coralline algae grow in the dark by using carbohydrate reserves (32) and CO_2 dark assimilation (33). Despite these differing growth strategies calibration indicates both summer and winter adherence to the Mg-temperature relationship (20) and also confirms temperature controlled replacement of Ca by Mg within the crystal lattice rather than the Mg being present as an associated organic component (14).

In this study, spectral analysis reveals significant (99% confidence level) shallow-water algae-derived in situ temperature frequencies of 64.8, 4.3, 2.8 and 2.1 years per cycle between 1431–2006 (the longest uninterrupted time-series data available) on the west coast of Scotland (Fig. 2). As oscillations are not clearly resolved prior to 1700 (Fig. 1) this may indicate temporal instability in marine temperature oscillations in the North East Atlantic at centennial scales. Mg/Ca derived marine SST correlate well with atmospheric temperatures (20), suggesting that both may exhibit similar oscillations. The 50–100 year climate oscillations observed in the Atlantic climate system (10, 34) are only for records extending to the 1800s but their presence does confirm that similar oscillations occur in both Atlantic seawater and the Atlantic climate system. Similar 50–100 year in situ shallow-water sea temperature oscillation longevity has been observed in coral-derived SST reconstructions of Atlantic low latitudes (29) suggesting that, whereas those oscillations are spatially widespread and contemporaneous within the Atlantic Ocean, their temporal instability may be an Atlantic-wide phenomenon. The 4.3 year signal corresponds to NAO (35) and El Niño Southern Oscillation (36) timescales whereas the biennial peaks are close to the Nyquist frequency and thus most likely of analytical rather than climatic origin (37).

Winter AMO and algae-derived in situ winter temperature both show significant coherence at 64–65, 45.1, and 2.2 year frequencies (Figs. 1 and 2) between 1856–2005 (the longest suitable AMO time series available). The 64–65 year period is also present in the algae-derived in situ winter temperature whereas the biennial period is close to the Nyquist frequency. This relationship with the AMO is to be expected as AMO is defined by SST (38). There is an absence of any upward trend in the AMO (as present in temperature between 1856–2005) as the AMO is calculated from detrended SST data. The similarity between algae-derived in situ temperature and the AMO (and thus SST) is important as the AMO may be correlated to the AMOC (39), which is thought to be driven by the thermohaline circulation (THC) (10). It thus appears that shallow-water algae-derived in situ temperatures recorded by red coralline algae on the west coast of Scotland may also be a record of THC change. Multidecadal oscillatory modes in SST (and presumably in situ temperature) and THC have been attributed to both the response of the atmosphere to extratropical SST anomalies and oceanic responses to stochastic surface flux forcing (10) whereas lower frequency (annual-decadal) temperature variability, as also observed in coral (29) and tree-ring (6) records is likely to be caused by volcanism, greenhouse gases, solar activity, and atmospheric aerosols (e.g., ref. 40). At longer temporal scales the pre-1700 absence of the AMO may be partly due to reduced AMOC transport during the LIA (41) and thus this record suggests that the AMOC transport may have increased from as early as 1700 in the North Atlantic compared to 1850 at lower Atlantic latitudes.

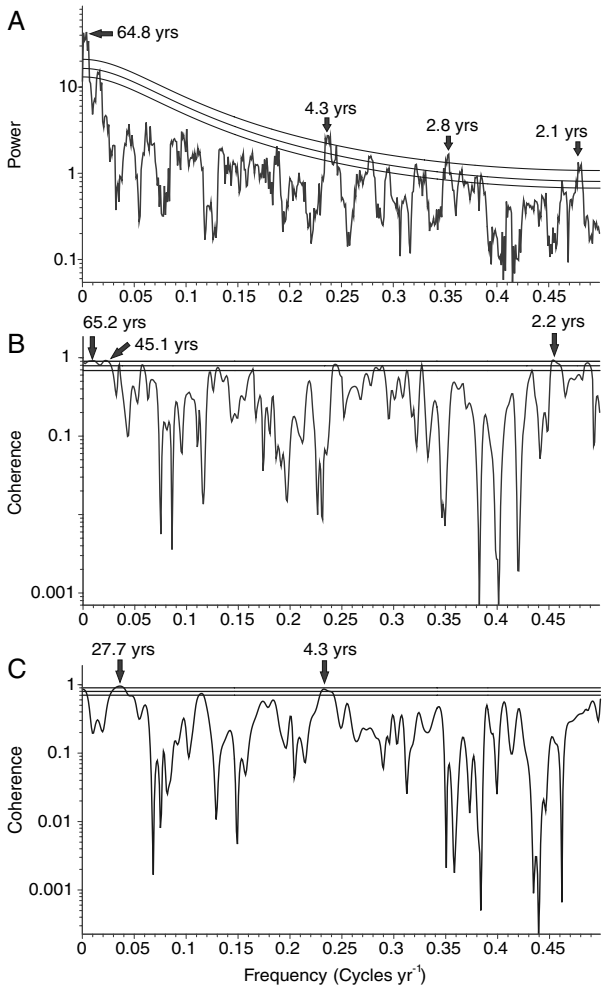

Fig. 2. Algae-derived in situ temperature periodicity. (*A*) Adaptively weighted MTM spectrum of the annual algae-derived in situ temperature at Loch Sween, Scotland from 1431 to 2006 (bandwidth parameter is $p = 2$ and $K = 3$ eigentapers were used). (*B*) Spectral coherence between algae-derived in situ winter temperature and winter Atlantic Multidecadal Oscillation index from (38) between 1859–2006 (bandwidth parameter is $p = 2$ and $K = 3$ eigentapers were used). (*C*) Spectral coherence between algae-derived in situ winter temperature and winter North Atlantic Oscillation index from (45) between 1900–2006 (bandwidth parameter is $p = 2$ and $K = 3$ eigentapers were used). In all plots the 90 (*Bottom*), 95 (*Middle*) and 99 (*Top*) % significance levels are shown by curves/lines. The periods (years cycle^{-1}) of signals significant at the 99% level are indicated.

Winter NAO and algae-derived in situ winter temperature both show significant coherence at 27.7 and 4.3 year frequencies (Figs. 1 and 2) between 1900–2005 (the longest suitable NAO time series available). These periods are very similar to those observed in winter NAO reconstruction using *Arctica islandica* (29–32 and 7–9 years) in the Norwegian Sea (42) as well as coherence between NAO and coral-derived Sr/Ca time series (3–5 years) from Bermuda (35). Coherence between proxy-derived in situ temperature and NAO is most likely observed because the NAO drives winter climate variability over Europe and eastern North America (43) and also because SSTs from the North Atlantic correlate with NAO at annual and decadal scales (44).

Thus the influences of both winter AMO and winter NAO appear to be recorded in the algal-derived reconstruction of shallow-water in situ temperatures on the west coast of Scotland. Whereas the NAO exerts most dominance on atmospheric winter temperatures over the East Atlantic and Europe (45), marine temperatures in the Atlantic Ocean are thought to be the dominant influence on summer atmospheric climate in the United Kingdom (9). As signals from both the winter AMO and winter NAO are present in the winter algae-derived in situ temperatures it is likely that both the AMO and NAO play a role in controlling winter temperatures on the west coast of Scotland. This observation has significance for seasonal scale climate projections over the next century in Northern Europe.

Since continuous plankton recorder sampling began in 1958 *C. finmarchicus* abundances have fallen from 15 to 4 relative abundance units with a notable peak occurring in 1979 (Fig. 3). Here, a significant negative relationship between log stabilized *C. finmarchicus* abundances and summer algae-derived in situ temperature was observed (Fig. 4) (Raw:

$$\mathrm{Log(Cfin)} = -0.27 * \mathrm{SumIST} + 7.78 \quad [1]$$

($R^2 = 0.28$, $p < 0.001$, $\mathrm{SE}_b \pm 0.06$, $\mathrm{SE}_a \pm 0.98$), and detrended:

$$\mathrm{Log(Cfin + 12)} = -0.17 * \mathrm{SumIST} + 6.35 \quad [2]$$

($R^2 = 0.19$, $p = 0.002$, $\mathrm{SE}_b \pm 0.01$, $\mathrm{SE}_a \pm 0.76$). As *C. finmarchicus* is most sensitive to temperature increases in early summer (25), which are partly controlled by the NAO (46), and the current study shows enhanced summer warming since the LIA, it is likely that *C. finmarchicus* is more sensitive to temperature rises than previously thought. Projections also suggest this, showing that *C. finmarchicus* abundances will continue to decline in response to increasing summer temperatures between 2006–2040 with the 2030–2039 mean abundance (3.3) being significantly lower than the 1995–2004 mean abundance (4.6) (Fig. 2) ($F_4 = 6.94$, $p = 0.017$). Thus increased summer warming on the west coast of Scotland may exacerbate the decline in *C. finmarchicus* abundance.

Marine fin-fish fisheries undergo sudden and significant changes in productivity that are often associated with lower-trophic levels (47). Such changes can impact fish stocks both directly (higher temperatures create greater energetic demands) and indirectly (phenological fall in available food) (48). Cod recruitment covaries positively with phytoplankton and zooplank-

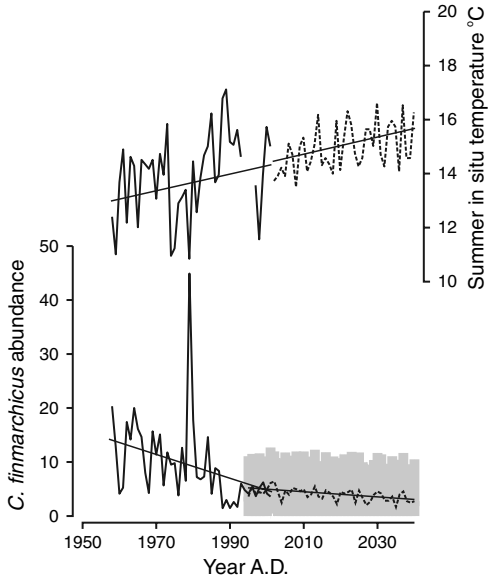

Fig. 3. Historic and projected in situ temperature and *C. finmarchicus* abundance. (*A*) Historic algae-derived in situ temperature time series (solid) and projected in situ temperature (dashed) obtained from ref. 19. (*B*) Historic *C. finmarchicus* abundance (solid) on the west coast of Scotland collected using a continuous plankton recorder (CPR). Abundance is on a semiquantitative relative scale of zooplankton per unit volume of water sampled by the CPR. Projected *C. finmarchicus* abundance (dashed) using function [**1**]. Linear trendlines are indicated by straight black lines.

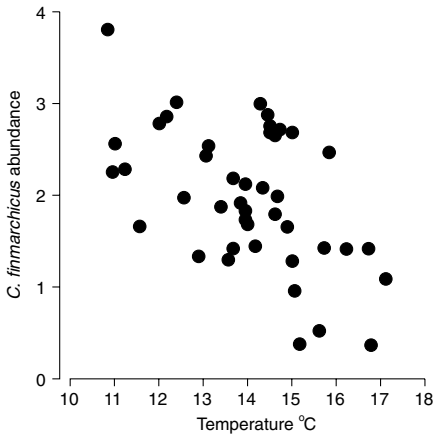

Fig. 4. Relationship between annual log (natural) *C. finmarchicus* abundance and summer algae-derived in situ temperature on the west coast of Scotland between 1956 and 2001 with 0 years lag.

ton (*C. finmarchicus* and *Calanus helgolandicus*) abundance due to reduced food (zooplankton availability and quality) (26). Since 1958 increasing temperatures have reduced the quality of zooplanktonic food available for larval/juvenile cod [progressive substitution of *C. finmarchicus* by *C. helgolandicus* at higher temperatures (25)], mediated by changes in water column stratification (49, 50), leading to poor recruitment to adult populations in the North Sea (26). In addition, decline in food availability has exacerbated the decline of European cod stocks due to overfishing (7). Added variability in cod recruitment also exists as a consequence of stock specific responses to: (*i*) temperature [e.g., stocks at different positions in cod's distributional range responding differently (51) and/or changing their spawning locations (52)], (*ii*) wind and current induced changes in the distribution of cod eggs and larvae (53) and (*iii*) variable responses to NAO (46, 54). Thus whereas in certain areas warming climate will lead to increased fishery yields (18) it appears that cod yields in the East Atlantic may be altered as a consequence of enhanced summer warming of waters at the time when their food, *C. finmarchicus*, is most sensitive to those changes. Such fluctuations in fish stocks have major economic and social consequences (7) and thus a detailed understanding of climate-induced changes, such as the inclusion of ecological knock-on effects (55), is required.

Conclusions

As global warming begins to represent a risk to global food security on land (56), marine fish stocks are also starting to dwindle (7). Enhanced increases in shallow-water marine summer temperatures observed here, have a negative effect on *C. finmarchicus* abundance in summer when it is most sensitive to temperature. As *C. finmarchicus* is a key prey item for cod this may have detrimental effects higher up the food web. We thus need to further understand if summers will continue to warm more than winters with respect to seasonal climate projections, the stability of the marine climate system and the knock-on effects these synergistic factors will have on fisheries and marine food security.

Materials and Methods

Algal Collection. SCUBA (self-contained underwater breathing apparatus) was used to collect a 20 × 46 cm core through a *L. glaciale* deposit in Loch Sween (56°01.99′N 05°36.13′W) on the west coast of Scotland in January 2007. Live *L. glaciale* on the surface of the deposit protected the core top from disturbance. The core was frozen and sectioned longitudinally; each half was sectioned into 2 cm horizons. To avoid edge effects of the coring process each horizon was recored using a 6 cm diameter core. *L. glaciale* thalli were picked from each horizon and washed. The longest thalli were selected for further analysis.

Rangefinder Dates. Five thalli were selected for radiocarbon rangefinder dating. For each thallus, a branch tip attached directly to the section used in Mg/Ca determination, and containing approximately 20 bands (years of growth), was selected for analysis. Each sample was sonicated to remove any ground-in material and analyzed whole. Accelerator mass spectrometry radiocarbon dating was conducted at the Scottish Universities Environmental Research Centre and adjusted by 405 ^{14}C years for the marine reservoir effect (57) (Table 1).

Sample Analysis. All analyses were conducted on a Cameca SX100 electron microprobe at the School of Geosciences, University of Edinburgh. Parallel transects ($n = 2$) were made along the length of each thallus. Along each transect, spot analyses (20 μm diam.) simultaneously recording Mg, Ca, and Sr were made at 20 μm steps [electron microprobe conditions: acceleration voltage: 10 kV, beam current: 4 nA, dwell time: 20 sec (see (20) for detailed conditions)]. Samples were imaged using SEM (FEI Quanta 200 F) and any spot analyses that were taken on growth irregularities were rejected (82 of the 12,888 analyses). Remaining values from the 2 transects were averaged to generate a Mg/Ca (molar) time-series. As *L. glaciale* band annually (20), band counting/imaging was used to correspond individual bands to annual peaks and troughs in the Mg/Ca time series that corresponded to maximum and minimum temperatures in individual years (e.g., as in Fig. S1). For the live collected specimens, this process enabled absolute dates to be assigned to each peak/trough. For validation of analytical technique , see *SI Text* and Fig. S2.

Combined Chronology. Six thalli were used as anchor points in construction of the combined chronology; a core top thallus provided the 0 year (as it was live on collection) and 5 other thalli provided radiocarbon dates. Twenty seven (including anchors) Mg/Ca time series were available; each from an individual thallus. Each time series was presented as both summer maximum and winter minimum molar Mg/Ca [maximum Mg is deposited during summer (20)]. These were detrended (least-squares regression) to remove any effects of band width on the number of Mg/Ca readings yr^{-1}, and hence resolution, when determining the chronology. The anchor point thalli were used to give all other thalli an estimated age (using interpolation). To further refine the age of each thallus, and thus the accuracy of the chronology, the detrended summer Mg/Ca time series determined from each thallus was cross correlated (average overlap = 64 years) with Mg/Ca time series for thalli that grew at similar times (estimated from interpolated age). Relative lagged ages determined by the cross correlation were only accepted if all the following criteria were met (*i*) correlation coefficient $r >= 0.36$ ($p < 0.001$) (58), (*ii*) Gleichlaufigkeit, GLK >= 65% (59), and (*iii*) Baillie–Plicher t value, $t_{BP} >= 3.6$ (60).

The combined use of radiocarbon dating and dendrochronological techniques allows for a chronology in which no ages are based only on interpolation thus reducing uncertainty introduced by interpolation as well as error associated with the radiocarbon dates. Thus the maximum error on any ages determined will be $t \pm 40$ y (the error on radiocarbon dates) plus/minus any interpolation error (≤14 y) whereas the minimum error will be 0 years (the best age determined using cross correlation). As three filtering criteria were used to determine cross correlation significance, it is likely that age model error falls well below the 54 year maximum and is probably nearer 0 years. It is unlikely there is error on the 1857–2006 ages as thalli that grew during these years were live on collection thus are absolutely dated, this is important as these are the years during which comparisons with absolutely dated zooplankton abundance are made.

Mg-Temperature Relationship. The Mg-temperature relationship: $Mg/Ca(molar) = 0.013\ IST(°C) + 0.04$ (IST = in situ temperature, Mg/Ca = molar Mg/Ca ratios in *L. glaciale*, $R^2 = 0.93$, $p < 0.001$, $SE_b \pm 6.5^{-4}$,

Table 1. Radiocarbon data for *L. glaciale* samples from Loch Sween, Scotland

Sample code	Depth (cm)	^{13}C relative to VPDB (‰)	Age	Year
SUERC-16011	8–10	−6.7	Modern	Pre 1950 AD
SUERC-16013	14–16	−6.9	Modern	Pre 1950 AD
SUERC-16005	26–28	−4.1	320 ± 40	1668 ± 40
SUERC-16006	30–32	−12.0	355 ± 40	1651 ± 40
SUERC-16012	44–46	−3.9	630 ± 40	1376 ± 40

Depth denotes the section depth down from top of live surface thalli, sediment depth begins ~8 cm below thallus surface. Ages are given as conventional ^{14}C yr BP with analytical error of $\pm 1\sigma$.

$SE_a \pm 6^{-3}$, equivalent error on reconstruction = ±0.5 °C) was determined using measured in situ temperature, the calibration site, technique, and validation in ref. 20 (Fig. S1). Two temperature time series were constructed, for (*i*) maximum summer temperature and (*ii*) minimum winter temperature. Fieller's Theorem was used to propagate errors. A gap is present in the time series during 1388–1405 due to the absence of multiple thalli growing during that period. Occasional individual gaps are also present when analyses in all thalli representing a particular time happened to fall on a growth irregularity and were rejected. ANCOVA (assumptions met) was used to compare temperatures between temporal bins.

Spectral Analysis. Multitaper method (MTM) spectral estimation (37, 61, 62) was conducted to estimate the winter algae-derived in situ temperature variability period. Winter temperatures were used as these gave a longer uninterrupted time series than summer temperatures. The MTM bandwidth parameter is $p = 2$ and $K = 3$ Slepian eigentapers were used. Confidence intervals were determined relative to a red noise AR(1) background. Comparison of algae-derived in situ temperature time series with the winter AMO and winter NAO time series was conducted using Magnitude-Squared Coherence—the frequency domain analogue of correlation (62, 63). For both the AMO and NAO the longest suitable time series available were used. The same bandwidth parameter and eigintaper were used as in MTM analysis. In all cases only signals significant at the 99% level were considered. Analyses were conducted on detrended time series (spline/linear model residuals) that were detrended separately.

Temperature-Zooplankton Relationships ***Data sources.*** Historic sea water temperatures were algae-derived in situ temperature time-series developed during the current investigation. Projected SSTs from 2000–2040 for 57°07′53″N 08°12′60″W were obtained from (19) and were developed under an SRES-A2 scenario. *Calanus finmarchicus* abundance (semiquantitative relative scale; e.g., number of zooplankton per unit volume of water sampled) data were collected using a Continuous Plankton Recorder in Area C4 (inshore west coast Scotland) and provided by The Sir Alister Hardy Foundation for Ocean Science (www.sahfos.ac.uk).

Data preparation and relationships. Residuals of each time series were obtained from linear models (variable ~ time). Remaining autocorrelation was removed by fitting successively higher order Autoregressive Integrated Moving Average models to each input variable (64). All analyses were conducted on the log stabilized residuals.

Model validation and projection. Temperature-zooplankton relationships were determined using models constructed from ~66% of the available time-series data (1958–1987). Those relationships were used to project the zooplankton abundance over the same period as the remaining 33% of the time series (1988–2001) providing projected and actual abundance time series over the period 1988–2001. Projective capacity was validated by regressing the difference between actual zooplankton abundance and projected zooplankton abundance on sums of actual and projected zooplankton abundance (65) between 1988–2001. *C. finmarchius* abundance was projected to 2040 using relationships [**1**] and [**2**]. The projection is useful for detecting changes in trend at decadal scales, however, is not suitable for detecting subannual patterns as error propagation makes subdecadal patterns hard to interpret. This can been observed in the small step change between proxy-derived and modeled temperatures at annual scales (Fig. 3) whereas the linear trendlines, representative of temperature/abundance at decadal scales, are temporally coherent. In addition, the annual step change is not of concern at decadal scales as the variability of modeled temperature is well within the variability of proxy-derived temperature (Fig. 3). Repeated measures ANOVA (assumptions met) was used to compare *C. finmarchicus* abundances at different temporal points.

Statistical analysis. Mg/Ca cross dating was conducted using CDendro (Cybis Elektronik & Data), spectral estimation was conducted using kSpectra Toolkit (Spectraworks, www.spectraworks.com) and all other analyses were conducted using R v2.10 (66).

ACKNOWLEDGMENTS. Thanks to Peter Chung, Chris hayward, John Faithful, Maggie Cusack, Marian Scott, and Vernon Phoenix for help with sample collection, analysis, and constructive suggestions. Thanks also to the University Marine Biological Station Millport dive team, the Scottish Universities Environmental Research Centre, and The Sir Alister Hardy Foundation for Ocean Science. This research was made possible by Grants NERC NE/D008727 and Royal Society of Edinburgh/Scottish Government RSE 48704/1.

1. Luterbacher J, Dietrich D, Xoplaki E, Grosjean M, Wanner H (2004) European seasonal and annual temperature variability, trends, and extremes since 1500. *Science* 303:1499–1503.
2. Mann ME, Bradley RS, Hughes MK (1998) Global-scale temperature patterns and climate forcing over the past six centuries. *Nature* 392:779–787.
3. Goosse H, Renssen H, Timmermann A, Bradley RS, Mann ME (2006) Using paleoclimate proxy-data to select optimal realisations in an ensemble of simulations of the climate of the past millennium. *Clim Dynam* 27:165–184.
4. Luterbacher J, et al. (2002) Extending North Atlantic Oscillation reconstructions back to 1500. *Atmos Sci Lett* 10.1006/asle.2001.0044.
5. Mann ME, et al. (2003) On past temperatures and anomalous late-20th century warmth. *EOS Trans Am Geophys Union* 84:256–257.
6. Casty C, Wanner H, Luterbacher J, Esper J, Bohm R (2005) Temperature and precipitation variability in the european Alps since 1500. *Int J Climatol* 25:1855–1880.
7. Brander K (2010) Impacts of climate change on fisheries. *J Marine Syst* 79:389–402.
8. Dong BW, Sutton RT (2005) Mechanism of interdecadal thermohaline circulation variability in a coupled ocean-atmosphere GCM. *J Climate* 18:1117–1135.
9. Sutton RT, Hodson DLR (2005) Atlantic Ocean forcing of North American and European summer climate. *Science* 309:115–118.
10. Delworth TL, Mann ME (2000) Observed and simulated multidecadal variability in the Northern Hemisphere. *Clim Dynam* 16:661–676.
11. D'Arrigo R, Wilson R, Liepert B, Cherubini P (2008) On the "Divergence Problem" in Northern Forests: A review of the tree-ring evidence and possible causes. *Glob Planet Change* 60:289–305.
12. Schone BR, et al. (2005) Climate records from a bivalved Methuselah (*Arctica islandica*, Mollusca; Iceland). *Palaeogeog Palaeoclim Palaeoecol* 228:130–148.
13. Weidman CR, Jones GA, Lohmann KC (1994) The long-lived mollusc *Arctica islandica*: A new palaeoceanographic tool for the reconstruction of bottom temperatures for the continental shelves of the northern North Atlantic Ocean. *J Geophys Res* 99:18,305–18,314.
14. Kamenos NA, Cusack M, Huthwelker T, Lagarde P, Scheibling RE (2009) Mg-lattice associations in red coralline algae. *Geochim Cosmochim Acta* 73:1901–1907.
15. Cohen AL, Owens KE, Layne GD, Shimizu N (2002) The effect of algal symbionts on the accuracy of Sr/Ca paleotemperatures from coral. *Science* 296:331–333.
16. Shirai K, et al. (2005) Deep-sea coral geochemistry: Implication for the vital effect. *Chem Geol* 224:212–222.
17. Cushing DH (1982) *Climate and Fisheries* (Academic Press, London) p 294.
18. Brown CJ, et al. (2010) Effects of climate-driven primary production change on marine food webs: Implications for fisheries and conservation. *Glob Change Biol* 16:1194–1212.
19. Stendel M, Schmith T, Roeckner E, Cubasch U (2004) IPCC_ECHAM4OPYC_SRES_A2_MM. *World Data Centre for Climate* 10.1594/WDCC/IPCC_EH4_OPYC_SRES_A2_MM.
20. Kamenos NA, Cusack M, Moore PG (2008) Red coralline algae are global paleothermometers with bi-weekly resolution. *Geochim Cosmochim Acta* 72:771–779.
21. Halfar J, Zack T, Kronz A, Zachos JC (2000) Growth and high resolution palaeoenvironmental signals of rhodoliths (coralline red algae): A new biogenic archive. *J Geophys Res* 105:22,107–122,116.
22. Kamenos NA, Law A (2010) Temperature controls on coralline algal skeletal growth. *J Phycol* 46:331–335.
23. Foster MS (2001) Rhodoliths: Between rocks and soft places. *J Phycol* 37:659–667.
24. Taylor AH, Allen JI, Clark PA (2002) Extraction of a weak climatic signal by an ecosystem. *Nature* 416:629–632.
25. Planque B, Fromentin JM (1996) *Calanus* and environment in the eastern North Atlantic. 1. Spatial and temporal patterns of *C. finmarchicus* and *C. helgolandicus*. *Mar Ecol Prog Ser* 134:101–109.
26. Beaugrand G, Brander KM, Lindley JA, Souissi S, Reid PC (2003) Plankton effect on cod recruitment in the North Sea. *Nature* 426:661–664.
27. Mann ME, et al. (2009) Global signatures and dynamical origins of the Little Ice Age and Medieval Climate Anomaly. *Science* 326:1256–1260.
28. Kreutz KJ, et al. (1997) Bipolar changes in atmospheric circulation during the Little Ice Age. *Science* 277:1294–1296.
29. Saenger C, Cohen AL, Oppo DW, Halley RB, Carilli JE (2009) Surface-temperature trends and variability in the low-latitude North Atlantic since 1552. *Nat Geosci* 2:492–495.
30. Cook ER, D'Arrigo RD, Mann ME (2002) A well-verified, multiproxy reconstruction of the winter North Atlantic Oscillation index since AD 1400. *J Climate* 15:1754–1764.
31. Kerr RA (2000) A North Atlantic climate pacemaker for the centuries. *Science* 288:1984–1986.
32. Freiwald A, Henrich R (1994) Reefal coralline algal build-ups within the Arctic circle: Morphology and sedimentary dynamics under extreme environmental seasonality. *Sedimentology* 41:963–984.
33. Kremer BP (1981) Apsects of carbon metabolism in marine macroalgae. *Oceanogr Mar Biol Annu Rev* 19:41–95.
34. Schlesinger ME, Ramankutty N (1994) An oscillation in the global climate system of period 65–70 years. *Nature* 367:723–726.
35. Goodkin NF, Hughen KA, Doney SC, Curry WB (2008) Increased multidecadal variability of the North Atlantic Oscillation since 1781. *Nat Geosci* 1:844–848.
36. Mann ME, Park J (1994) Global-scale modes of surface temperature variability on interannual to century timescales. *J Geophys Res* 99:25819–25833.

37. Mann ME, Lees JM (1996) Robust estimation of background noise and signal detection in climatic time series. *Climate Chang* 33:409–445.
38. Enfield DB, Mestas-Nunez AM, Trimble PJ (2001) The Atlantic Multidecadal Oscillation and its relationship to rainfall and river flows in the continental US. *Geophys Res Lett* 28:2077–2080.
39. van Oldenborgh GJ, te Raa LA, Dijkstra HA, Philip SY (2009) Frequency- or amplitude-dependent effects of the Atlantic meridional overturning on the tropical Pacific Ocean. *Ocean Sci* 5:293–301.
40. Andronova NG, Schlesinger ME (2000) Causes of global temperature changes during the 19th and 20th centuries. *Geophys Res Lett* 27:2137–2140.
41. Lund DC, Lynch-Stieglitz J, Curry WB (2006) Gulf Stream density structure and transport during the past millennium. *Nature* 444:601–604.
42. Schone BR, et al. (2003) North Atlantic Oscillation dynamics recorded in shells of a long-lived bivalve mollusk. *Geology* 31:1037–1040.
43. Hurrell JW, Kushnir Y, Ottersen G, Visbeck M, eds. (2003) *The North Atlantic Oscillation: Climatic Significance and Environmental Impact* (American Geophysical Union, Washington, DC).
44. Czaja A, Frankignoul C (2002) Observed impactof Atlantic SST anomalies on the North Atlantic oscillation. *J Climate* 15:606–623.
45. Hurrell JW (1995) Decadal trends in the North Atlantic Oscillation: Regional temperatures and precipitation. *Science* 269:676–679.
46. Fromentin JM, Planque B (1996) *Calanus* and environment in the eastern North Atlantic. 2. Influence of the North Atlantic Oscillation on *C. finmarchicus* and *C. helgolandicus*. *Mar Ecol Prog Ser* 134:111–118.
47. Mackas DL, Beaugrand G (2010) Comparisons of zooplankton time series. *J Marine Syst* 79:286–304.
48. Stenseth NC, et al. (2002) Ecological effects of climate fluctuations. *Science* 297:1292–1296.
49. Martinez E, Antoine D, D'Ortenzio F, Gentili B (2009) Climate-driven basin-scale decadal oscillations of oceanic phytoplankton. *Science* 326:1253–1256.
50. Dickson RR, Kelly PM, Colebrook JM, Wooster WS, Cushing DH (1988) North winds and production in the eastern North-Atlantic. *J Plankton Res* 10:151–169.
51. Planque B, Fredou T (1999) Temperature and the recruitment of Atlantic cod (*Gadus morhua*). *Can J Fish Aquat Sci* 56:2069–2077.
52. Deyoung B, Rose GA (1993) On recruitment and distribution of Atlantic cod (*Gadhus morhua*) off Newfoundland. *Can J Fish Aquat Sci* 50:2729–2741.
53. Dickson RR, Brander KM (1994) Effects of a changing windfield on cod stocks of the North Atlantic. *Cod and Climate Change—Proceedings of a Symposium*, Ices Marine Science Symposia, eds J Jakobsson et al. (Int Council Exploration Sea, Copenhagen), Vol 198, pp 271–279.
54. Ottersen G, Stenseth NC (2001) Atlantic climate governs oceanographic and ecological variability in the Barents Sea. *Limnol Oceanogr* 46:1774–1780.
55. Poloczanska ES, Hawkins SJ, Southward AJ, Burrows MT (2008) Modeling the response of populations of competing species to climate change. *Ecology* 89:3138–3149.
56. Battisti DS, Naylor RL (2009) Historical warnings of future food insecurity with unprecedented seasonal heat. *Science* 323:240–244.
57. Ascough PL, et al. (2004) Holocene variations in the Scottish marine radiocarbon reservoir effect. *Radiocarbon* 46:611–620.
58. Butler PG, et al. (2009) Accurate increment identification and the spatial extent of the common signal in five *Arctica islandica* chronologies from the Fladen Ground, northern North Sea. *Paleoceanography* 24:PA2210.
59. Schweingruber FH (1988) *Tree Rings: Basics and Applications of Dendrochronology* (Kluwer, Dordrecht, The Netherlands).
60. Miles D (1997) The interpretation, presentation, and use of tree-ring dates. *Vernacular Architecture* 28:40–56.
61. Ghil M, et al. (2002) Advanced spectral methods for climatic time series. *Rev Geophys* 40:3,1–3,41.
62. Thomson DJ (1982) Spectrum estimation and harmonic analysis. *Proceedings of the IEEE* 70:1055–1096.
63. Kuo C, Lindberg C, Thomson DJ (1990) Coherence established between atmospheric carbon-dioxide and global temperature. *Nature* 343:709–714.
64. Box GEP, Jenkins J (1976) *Time Series Analysis: Forecasting and Control* (Holden-Day, San Francisco), 2nd Ed.
65. Kleijnen JPC (1999) Validation of models: statistical techniques and data availability. *1999 Winter Simulation Conference Proceedings*, eds PA Farrington, HB Nembhard, DT Sturrock, and GW Evans pp 647–654.
66. RCoreDevelopmentTeam (2006) *The R Project for Statistical Computing* http://www.r-project.org/.